Digital-based analog processing in nanoscale CMOS ICs for IoT applications

Dual-Band Circularly Polarized MIMO DRA for Sub-6 GHz Applications

Sumer Singh Singhwal[1], Binod K. Kanaujia[2], Ajit Singh[3], Jugul Kishor[4], Ladislau Matekovits[5]*

[1] Department of Electronics and Communication Engineering, Uttrakhand Technical University, Dehradun, India, and Department of Electronics and Communication Engineering, HMR Institute of Technology and Management, Delhi, India
[2] School of Computational and Integrative Science, Jawaharlal Nehru University, Delhi
[3] B.T.K. Institute of Technology, Dwarahat, Uttarakhand, India
[4] Department of Electronics and Communication Engineering, JIMS Engineering Management Technical Campus Greater Noida, India
[5] Department of Electronics and Telecommunications, Politecnico di Torino, 10129 Torino, Italy
*Corresponding author email: ladislau.matekovits@polito.it

Abstract:
In this article, a dual-band circularly polarized Multiple-Input-Multiple-Output (MIMO) dielectric resonator antenna (DRA) is proposed for 3.5 GHz and 5.5 GHz bands, both being located under 6 GHz. Known as Sub-6 (or as mid-band), they provide good coverage and capacity in the newly targeted fifth-generation (5G) systems. The proposed structure consists of two ring DRAs (RDRAs) etched on a 0.8 mm thick RT Duroid substrate. Measured impedance bandwidths in broadside direction are 3.1 GHz-3.75 GHz (19%) and 5.3 GHz-5.6 GHz (9.4%) and circular polarization (CP) bandwidths are 3.425 GHz-3.6 GHz (5%) and 5.45 GHz-5.55 GHz (2%), respectively. CP is achieved by exciting HE modes using two probes placed orthogonaly to each other, i.e., at an azimuthal angular distance of 90°. Varying the lengths of the probe allows achieving the necessary time-phase quadrature between modes. Comparison between recent multi-band circularly polarized MIMO DRAs and proposed prototype has revealed that CP bandwidth in both bands is one of the highlighting advantages of the present configuration.

KEYWORDS: Circular polarization, Dielectric Resonator Antenna, Multiple-Input-Multiple-Output, 5G, Sub-6 GHz.

1 Introduction

The field of wireless communication is growing rapidly, to fulfill the need of high-speed data transfer applications. The 5G wireless communication system has been designed to support enhanced mobile broadband, ultra-reliability and low latency, massive machine type communication and fiber type speed to homes and businesses. It means 5G standards are defined in such a way to offer greater range of capability in comparison with previous generation mobile communications [1]. To support nationwide services, Sub-6 GHz band can use channel size from 50 MHz to 100 MHz. Multiple-Input-Multiple-Output (MIMO) antenna technology is a key concept used to enhance capacity of 5G networks because of its various advantages such as diversity performance and improved channel capacity [2]. In addition, the use of circular polarization (CP) in MIMO systems are also advantageous due to low polarization loss, less multipath interference, better performance and reliability [3]. There are various types of antennas to adopt MIMO functionality and out of these antennas, DRAs are the most promising ones due to their advantages such as high radiation efficiency, less surface wave loss and low ohmic losses [4]. Nowadays, dual frequency antennas are mostly desired because of increasing wireless applications. In the scientific literature, dual band MIMO DRAs are proposed, for example, in [5–10] but the discussed solutions refer to linearly polarized antennas. In [11] a tri-band dielectric resonator based hybrid antenna for WLAN/WiMAX application is reported. In this work, circular ring with T-shaped printed line produces dual hybrid radiating modes in cylindrical dielectric resonator antenna (CDRA). But advantages of CP in antennas swerved the researchers towards new domain of circularly polarized MIMO DRA. Very few articles [12–18] have been reported in this domain. In [12], the authors have proposed dual polarized triple band (2.213.13, 3.403.92, and 5.306.10 GHz) MIMO DRA for WLAN/WiMAX applications. The discussed configuration has achieved significant CP bandwidth for the upper band only. Reported gain in the three bands are 1.5 dBi, 4.2 dBi and 2.3 dBi, respectively. In [13], a dual port DR based circularly polarized MIMO antenna has been proposed for WLAN applications, however only simulated results are discussed. In [13], a corner truncated V-shaped DR has been utilized to obtain CP radiation and two symmetric orthogonal feed networks have been deployed to lessen mutual coupling between the ports. In [14], two self-complementary L-shaped DR based MIMO antennas have been reported with 5.16-6.30 GHz impedance bandwidth and 5.20-6.08 GHz axial ratio band width (ARBW). In [15], a dual port CDRA based MIMO antenna with dual sense polarization has been presented for WLAN applications. In [16], a hybrid technique has been employed using a parasitic patch at an optimized distance beside the conformal metal strip of the two identical rectangular DRAs in order to generate CP wave. In [17], two-element CP-DRA array has been implemented with electromagnetic band-gap (EBG) structure etched into the ground plane of the microstrip patch transmission line. In the best knowledge of authors, no work is reported related to dual-element, dual-band DRA based MIMO antenna with CP in both the operating bands. In [18], some of the authors of the present work has proposed the concept of CP agility in MIMO DRA for 5G applications.

In this article, a dual band compact MIMO DRA is proposed with CP operating in the

3.5 GHz and 5.5 GHz bands. *The structure consists of two ring DRAs excited by two arc-shaped line feeds and four conformal probes. The total substrate size is* $50x110mm^2$ *which makes it compact for sub-6 GHz band applications (3.5 GHz and 5.5 GHz) which includes WLAN, WiMAX and 5G communications. Main advantages of the proposed antenna are:* (i) *Ease of fabrication of DRs, the microstrip line feed and the defect ground structure (DGS),* (ii) *Compact in size with dual-elements on the substrate,* (iii) *CP bandwidth is available in both the operating bands. The major contribution of this dissemination is to give concept of dual band with circular polarization in both the bands with the help of ring DRAs in realization of MIMO antennas. Isolation is achieved by using polarization diversity as well as utilization of simple DGS. Impedance matching is fulfilled by applying arc shaped microstrip line feed structure.*

2 Antenna Structure and Theory

The geometry of the proposed antenna is shown in Fig. 1 and design parameters are shown in Table 1. The used substrate is RT Duroid with relative dielectric constant $\varepsilon_{rsub} = 2.33$, thickness W_{sub}=0.8 mm and $\tan\delta = 0.0012$. Moreover, Eccostock Hik bar with $\epsilon_{rdra} = 10$, $tan\delta = 0.001$ has been used as DRA material. The antenna structure comprises *i)* a (110×50 mm^2) sized rectangular substrate, *ii)* two arc shaped microstrip lines feed, *iii)* two conformal probes per RDRA with heights 9 mm and 15 mm, *iv)* two ring shaped DRAs, *v)* a DGS structure with a rectangle cut in the ground.

Table 1: Design Parameters

Parameter	Dimensions (in mm)	Parameter	Dimensions (in mm)
L	110	W	50
A	53.8	C	28.8
W1	2.4	W2	1.3
H1	9	H2	15
Hs	5	H	16.5
Ddra	25.5	R	8.5
Ws	2.4	Ls	50
Lf	21	Wsub	0.8
Din	5		

In this article, conformal probes have been chosen to excite the $HE_{11\delta}$ and $HE_{12\delta}$ modes having different resonant frequencies in the RDRA. Naturally comprehended conformal probe has been designed, optimized by using HFSS software, and experimentally proved with a promise for dual-band operation of the RDRA. In $HE_{11\delta}$ mode in the RDRA is excited by using probe feed technique, which provides good impedance matching. To realize

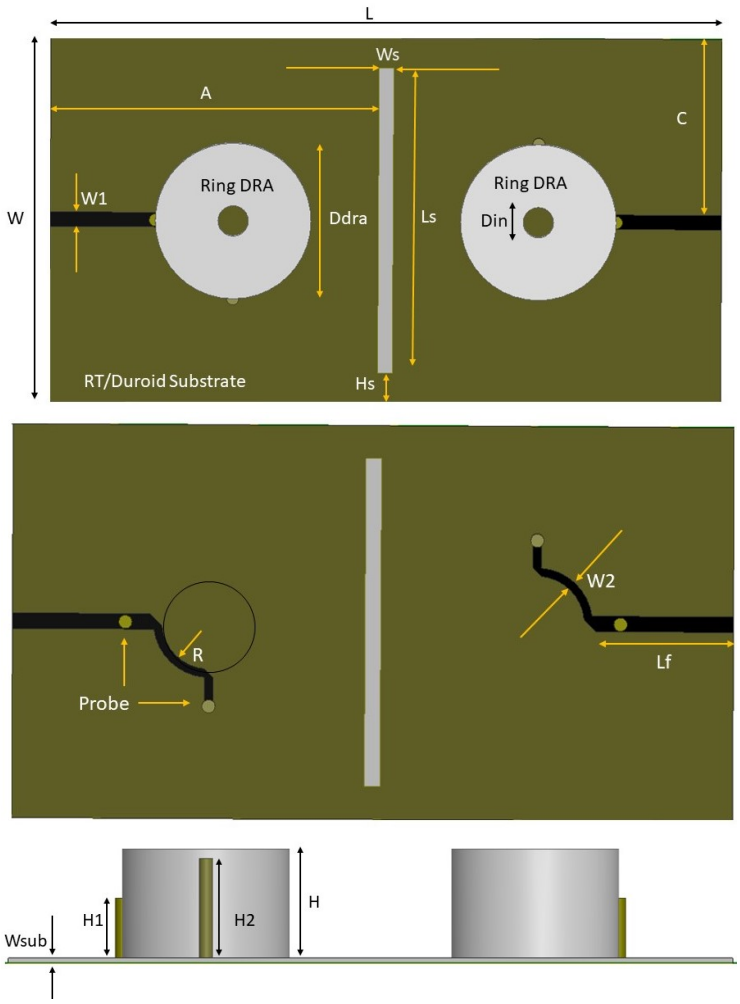

Figure 1: Antenna geometry with leading dimensions (numerical values are reported in Tab. 1). Top view (top), top view of the feeding circuit (center), side view (bottom).

the dual mode excitation (for the structure supporting both the modes) with a single feed requires a proper feed network, which excites two orthogonal modes at each frequency. The conformal feed consists of two probes, which excite two orthogonal components of fields with same magnitude and in time-phase quadrature in the RDRA. So, the conformal probe excitation is an easy and effective feed method where it is required to couple field energy between DRA and feed-line [19]. It should be relevant to note that the conformal probe feed structure should also helpful to realize CP. Principal of generation of CP states that, CP field can be attained in a DRA by exciting two orthogonal components of fields with same magnitude and in time-phase quadrature. Following this principal, in the proposed antenna, arc-shaped line feed provides orthogonality in field input and heights of probes decides time-phase quadrature relationship. Both the probes, as shown in Fig.1, have been placed on arc-shaped feed line. These probes excite orthogonal modes inside DRA because

each of them can generate both an x-polarized and y-polarized electric field lines. Time-phase quadrature relationship between both orthogonal field components is controlled by optimizing the heights of the two probes. Coupling of field components between the probe and RDRA, and impedance matching depends on the feed network configuration, which can be optimized by choosing different width of the arc-shaped line and feed line. Width of feed line and arc-shaped line corresponds to 50 Ω and 70 Ω characteristic line impedance, respectively. By adjusting the height of probes the $HE_{11\delta}$ mode in the RDRA can be excited. Conformal probe-1 excites $HE^{x}_{11\delta}$ mode while probe-2 excites $HE^{y}_{11\delta}$ mode. As a proof, two dips at 3.3 GHz and 3.6 GHz, respectively, in the S-parameter graph in Fig. 2 can be observed.

The values of ϵ_{reff} and H_{eff} are calculated by using following equations Eq. (1) and Eq. (2) [14].

$$\epsilon_{reff} = \frac{H_{eff}}{(H/\epsilon_{rCDRA}) + (W_{sub}/\epsilon_{rsub})} \tag{1}$$

$$H_{eff} = H + W_{sub} \tag{2}$$

The design equation used to calculate the resonant frequency of the CDRA is shown in Eq.(3) [4, 11].

$$f_{r(HE_{11\delta})} = \frac{18.963 \times 10^{8}}{\pi Dra\sqrt{\epsilon_{reff}+2}} \times \left[0.27 + 0.36\left(\frac{Ddra}{4H}\right) + 0.02\left(\frac{Dra}{4H}\right)^{2}\right] \tag{3}$$

The resonant frequency of the $HE_{12\delta}$ mode is approximated as 1.6 times of that of $HE_{11\delta}$ mode as shown in Eq.(4). The scaling ratio of 1.6 depends upon the aspect ratio (Ddra/2H) of CDRA as mentioned in [11, 20].

$$f_{r(HE_{12\delta})} = 1.6 \times f_{r(HE_{11\delta})} \tag{4}$$

The second resonance at 5.5 GHz is due to $HE_{12\delta}$ mode. Details about how to calculate the second resonance frequency band is also explained in [20]. Figure 2 shows simulated input scattering responses of the proposed antenna with RDRA, with CDRA and without DRA: the RDRA provides lower frequency band while upper frequency band is the combined effect of RDRA and conformal probes. The antenna with RDRA has improved impedance bandwidth, isolation and ARBW in comparison to antenna with CDRA. An optimization aiming to find the diameter of the hole in the RDRA has been performed using HFSS software. A rectangular slot is cut in the ground to increase isolation between ports. Figure 3 shows a comparison of isolation between ports with DGS and without DGS. Minimum isolation measured between ports in lower and upper operating band is -16.2 dB and -16.5 dB, respectively.

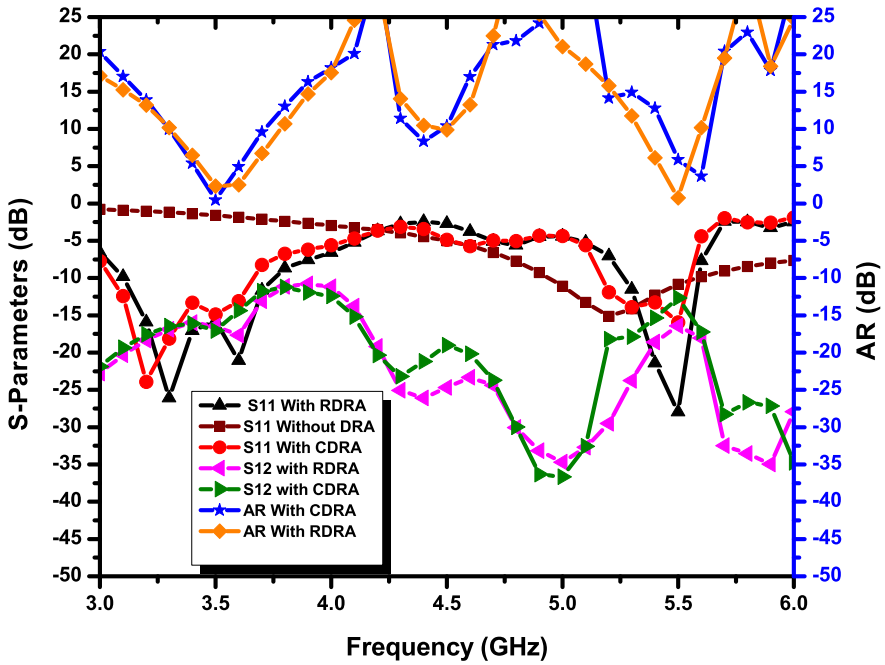

Figure 2: S-Parameters and ARBW comparison with RDRA, with CDRA and without DRA

3 Results and Validation

To validate the simulated results, a prototype of the proposed antenna has been fabricated, as shown in Fig. 4, and measured results have been compared to simulated counterparts. Simulated and measured input scattering parameters of proposed antenna are shown in Fig. 5, with measurement setup in anechoic chamber depicted in inset of the figure. The 3 dB ARBW for both bands are shown in Fig. 6. *Simulated and measured results are in good agreement with some reduced variations due to fabrication tolerance, soldering imperfections and due to usage of adhesive to stick on substrate. However, very minimal amount of adhesive is applied but effect of air layer in between DRA and substrate surface may result deviation in results which is depicted in Fig. 5 and Fig. 6.* Measured 10 dB impedance bandwidths are 3.1 GHz -3.75 GHz (19%) and 5.3 GHz -5.6 GHz (9.4%); the 3dB ARBWs are 3.425 GHz -3.6 GHz (5%) and 5.45 GHz -5.55 GHz (2%), respectively, in broadside direction. Isolation between ports at 3.5 GHz and 5.5 GHz have been measured to be equal to -16.2 dB and -16.5 dB, respectively.

Measured E- (left) and H-plane (right) radiation patterns at 3.5 GHz and 5.5 GHz are reported in Fig. 7 and Fig. 8, respectively: left hand CP wave dominates over right hand counterpart by acceptable margin. Figure 9 shows the surface current distribution on the ground plane to quantify isolation between ports at both the resonant frequencies. HE_{mmp} *mode is basically the hybrid mode, in which* E_Z *component is more dominant as compared*

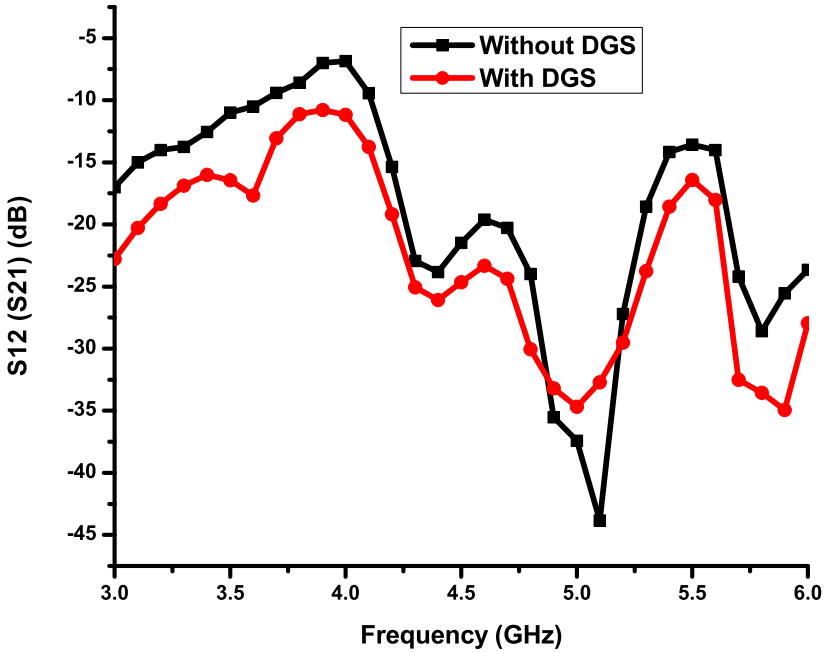

Figure 3: Effect of DGS on isolation between ports

to H_Z component. $HE_{11\delta}$ mode in CDRA indicates that there are the one full and one half wave variations in azimuthal and radial directions, respectively. Similarly, $HE_{12\delta}$ mode in CDRA indicates that there is the one full and two half wave variations in azimuthal as well as radial directions, respectively. δ indicates that the variation in axial direction (z) is in between the 0 and 1.Field distribution on the surface of the RDRA is shown in Fig. 10 which is approximately same as that of CDRA and this difference can be attributed due to air gap at the center. Table 2 shows a comparison between calculated, simulated and measured resonant frequencies of the DRA. It is observed that resonant frequencies for lower and upper bands corresponding to $HE_{11\delta}$ and $HE_{12\delta}$ modes in RDRA have drifted in comparison to that of CDRA.

MIMO performance has been evaluated by calculating $DG = 10\sqrt{1 - ECC^2}$ [21–23] and ECC using Eq. (5).

$$ECC = \frac{\left| \iint_{4\pi} \left[\overrightarrow{F_1}(\theta,\phi) * \overrightarrow{F_2}(\theta,\phi) \right] d\Omega \right|^2}{\iint_{4\pi} \left| \overrightarrow{F_1}(\theta,\phi) \right|^2 d\Omega \iint_{4\pi} \left| \overrightarrow{F_2}(\theta,\phi) \right|^2 d\Omega} \tag{5}$$

where $\overrightarrow{F_i}(\theta,\phi)$ is three dimensional field radiation pattern of the MIMO antenna when port-i is excited. Ω is solid angle and $*$ represents the Hermitian product operator. ECC

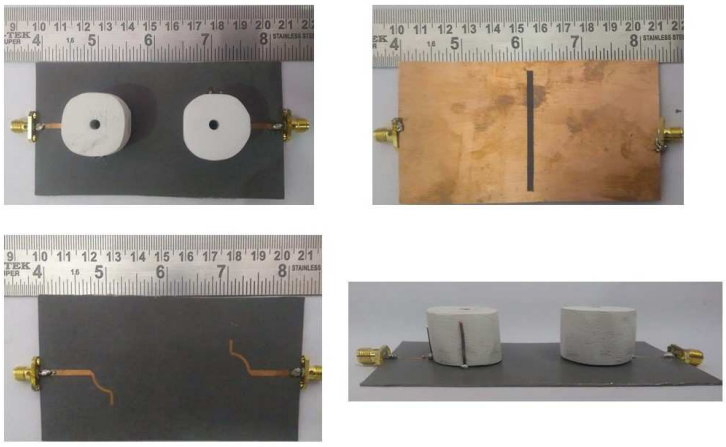

Figure 4: Photographs of the different parts of the fabricated prototype

shows the amount of channel isolation in a wireless communication link. In Table 3 a comparison between the performances of the proposed antenna and data available in the literature is reported.

Table 2: Comparison of Resonant Frequencies (GHz)

	Calculated f_r of CDRA	Simulated f_r of RDRA	Measured f_r of RDRA
Lower band	3	3.3 and 3.6	3.3 and 3.6
Upper band	4.8	5.5	5.5

Simulated and measured ECC and DG for lower and upper bands are shown in Fig. 11 and Fig. 12, respectively. ECC is well below 0.5 throughout the lower and upper operating bands and correlation coefficient (square root of ECC) is well below 0.3 as mentioned in [22, 24]. DG is above 9.8 dB for both the operating bands.

4 Conclusion

In this article, a dual-band MIMO ring dielectric resonator antenna with appreciated CP performance has been proposed that operates at 3.5 GHz and 5.5 GHz WiMAX bands. Measured ECC is below 0.5 and DG is above 9.8 dB for both bands. Measured impedance bandwidths are 19% and 9.4% and ARBWs are 175 MHz and 100 MHz in broadside direction at 3.5 GHz and 5.5 GHz resonant frequencies, respectively. It demonstrates CP in both bands. The size of antenna is also compact (110×50 mm^2) which makes it good choice for sub-6 GHz dual band applications.

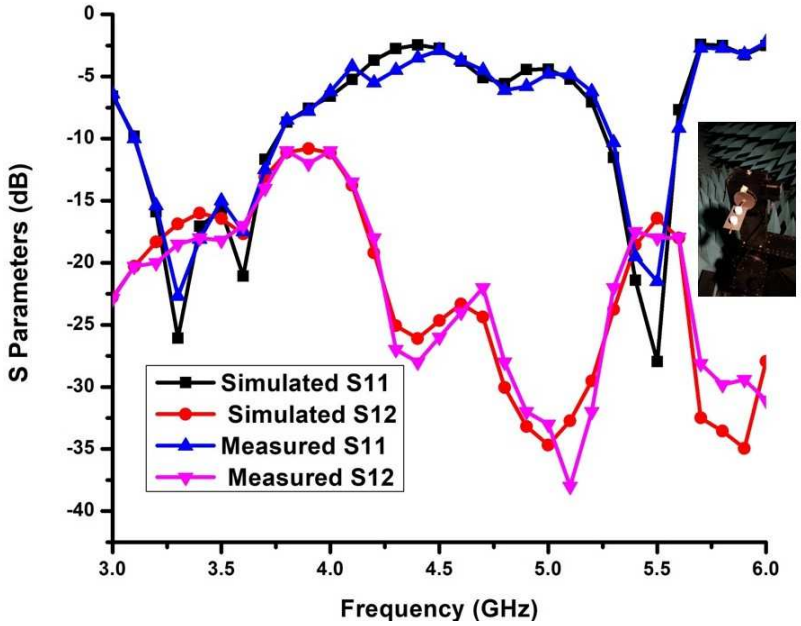

Figure 5: Simulated and measured S-Parameters of the proposed antenna

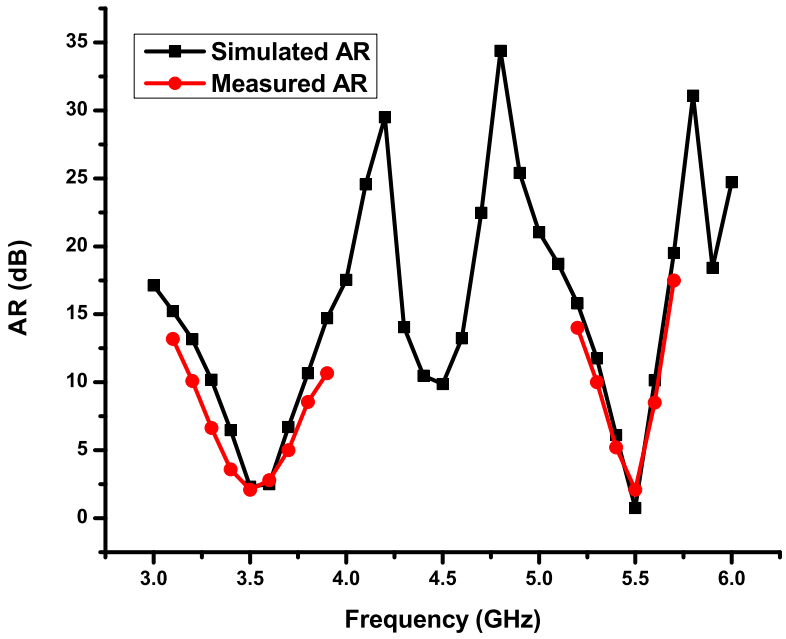

Figure 6: Simulated and measured ARBW of the proposed antenna

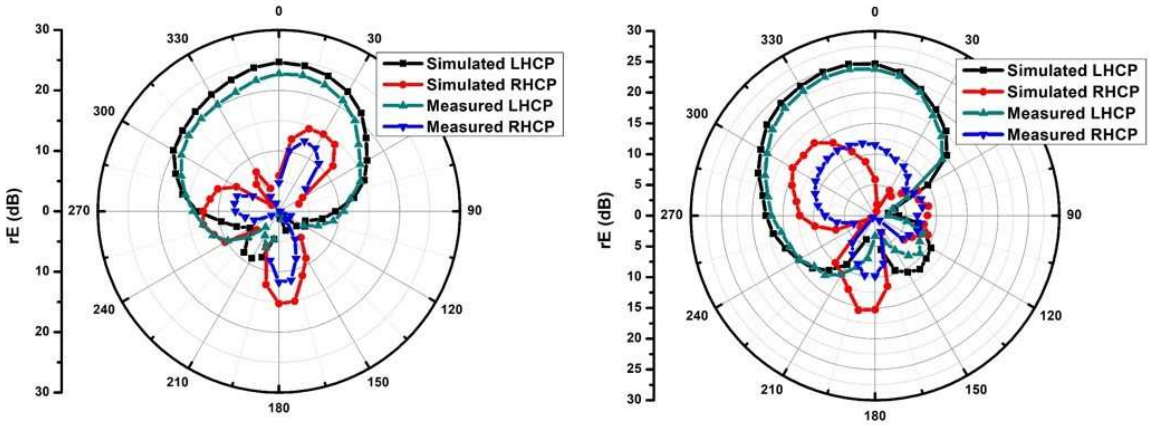

Figure 7: Simulated and measured radiation pattern of proposed antenna at 3.5 GHz E-plane (Left) and H-Plane (Right)

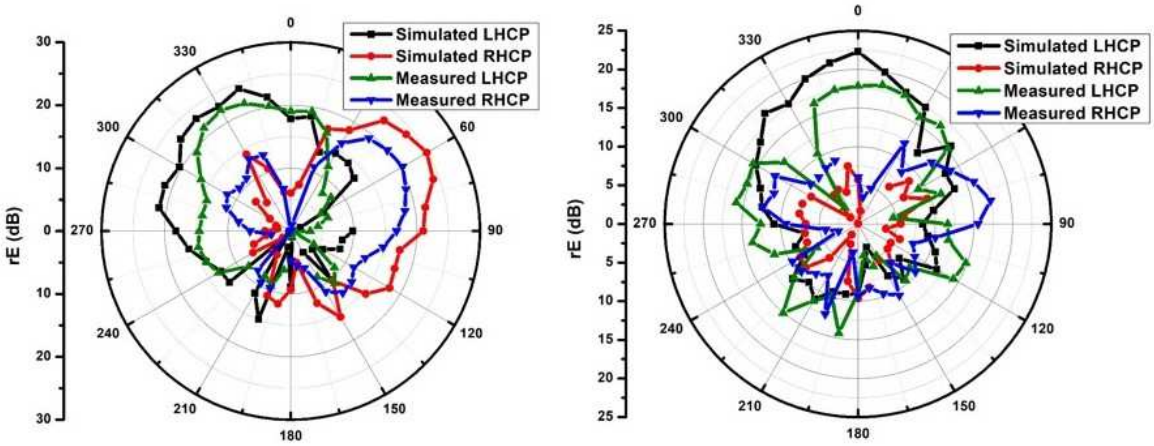

Figure 8: Simulated and measured radiation pattern of proposed antenna at 5.5 GHz E-plane (Left) and H-Plane (Right)

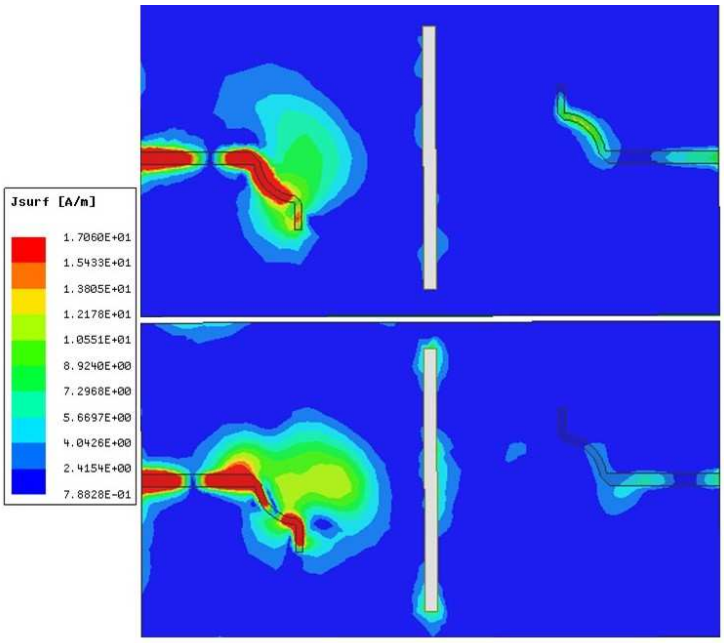

Figure 9: Surface current distribution on ground at 3.5 GHz (above) and at 5.5 GHz (below)

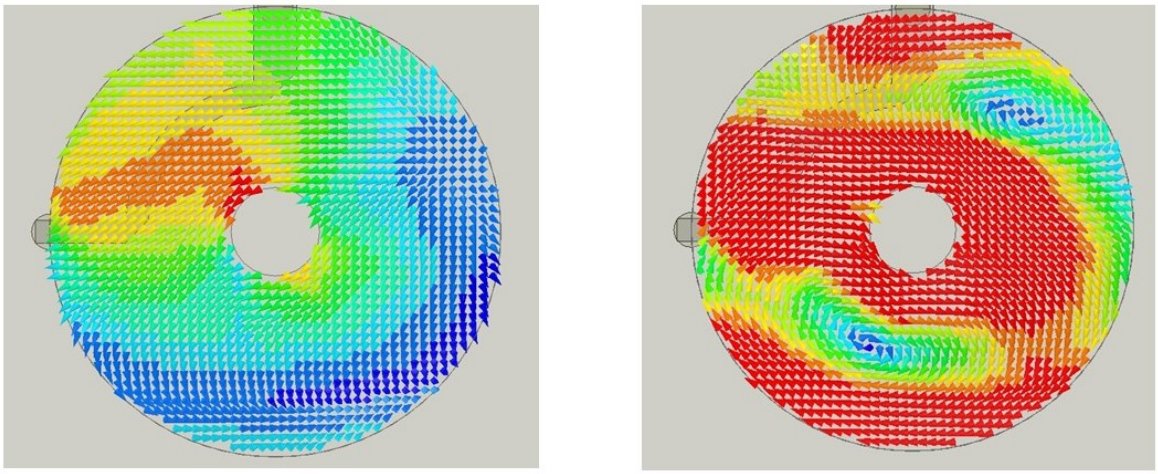

Figure 10: Field distribution on surface of RDRA at 3.5 GHz (Left) and 5.5 GHz (Right)

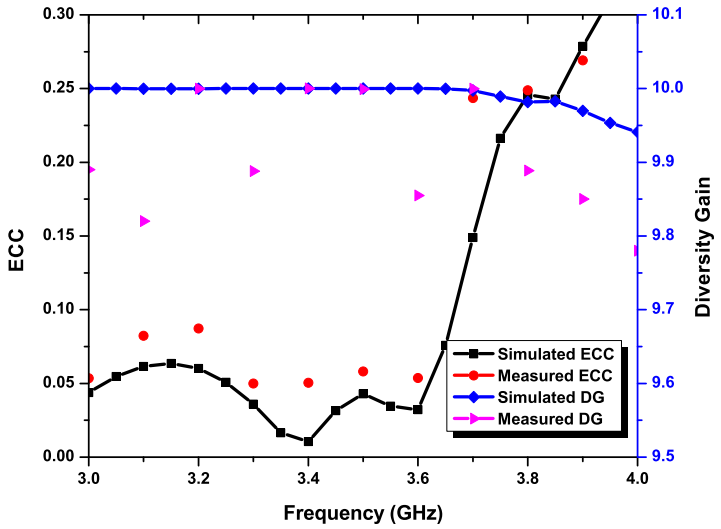

Figure 11: Simulated and measured ECC and DG for lower band

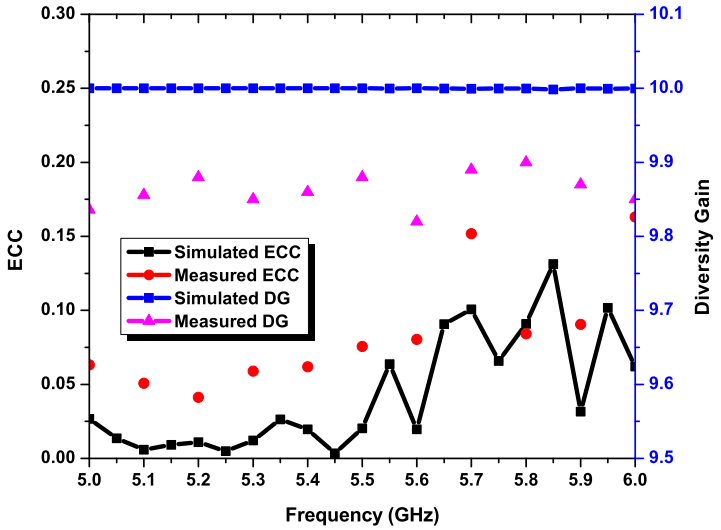

Figure 12: Simulated and measured ECC and DG for upper band

Table 3: Comparison of the proposed antenna with recently proposed CP MIMO DRA

Ref.	Impedance Bandwidth (GHz)	ARBW (GHz)	Gain (dBi)	Isolation (dB)
[12]	2.21-3.13, 3.4-3.92, 5.3-6.1	5.62-5.82	1.5, 4.1, 2.3	-20
[13]	4.89-5.42	5.16-5.38	5	-12
[14]	5.2-6.08	5.2-5.58	4	-19
[15]	5.25-6.25	not given	4.7	-25
[16]	3.5-4.95	3.58-4.4	6.2	-28
[17]	3.15-3.93	3.3-3.8 (simulated)	7.4 (simulated)	-24
[18]	3.12-3.9	3.26-3.45	7.3	-20
Proposed	**3.1-3.75, 5.3-5.6**	**3.425-3.6, 5.45-5.55**	**6.8,4.6**	**-16.5,-16.2**

Acknowledgement

Binod K. Kanaujia recognizes DBT & COE project funds for providing infrastructure support and DST-PURSE, Govt. of India & UPE II ID:340, JNU for providing support during the course of this investigation. Authors would like to be grateful to the Principal, G.B. Pant Engineering College Delhi, India, for giving access to the antenna measurement capacity at G.B.P.C.E. Delhi.

References

[1] Z. Ren, S. Wu, and A. Zhao, "Coexist design of sub-6 GHz and millimeterwave antennas for 5G mobile terminals," *Proc. Int. Symp. Antennas Propagat.*, Busan, South Korea, 2018, pp. 805806.

[2] H. Li, J. Xiong, Z. Ying and S.L. He, "Compact and low profile co-located MIMO antenna structure with polarisation diversity and high port isolation," *Electron. Lett.*, vol. 46, no. 2, pp. 108-110, 2010.

[3] F.A. Dicandia, S. Genovesi, and A. Monorchio, "Analysis of the performance enhancement of MIMO systems employing circular polarization," *IEEE Trans. Antennas and Propagat.*, vol. 65, no. 9, pp. 4824-4835, 2017.

[4] R.K. Mongia and P. Bhartia, "Dielectric resonator antennasA review and general design relations for resonant frequency and bandwidth," *Int. J. RF Microw Millim.-Wave Comput.-Aided Eng.*, vol. 4, no. 3, pp. 230-247, 1994.

[5] N.M. Nor, and M.H. Jamaluddin, "A dual band MIMO dielctric resonator antenna for WLAN application," *Jurnal Teknologi (Sciences & Engineering)*, vol. 77, no. 10, pp. 1-4, 2015.

[6] A. Sharma, A. Sarkar, A. Biswas, and M.J. Akhtar, "Dual-band multiple-input multiple-output antenna based on half split cylindrical dielectric resonator," *J. of Electromag. Waves and App.*, vol. 32, no. 9, pp. 1152-1163, 2018.

[7] A.A. Khan, M.H. Jamaluddin, J. Nasir, R. Khan, S. Aqeel, J. Saleem, and O. Owais, "Design of a Dual-Band MIMO Dielectric Resonator Antenna with Pattern Diversity for WiMAX and WLAN applications," *Progress in Electromagnetics Research M*, vol. 50, pp. 6573, 2016.

[8] A.A. Khan, R. Khan, S. Aqeel, J. Nasir, J. Saleem, and O. Owais, "Design of a dual-band MIMO dielectric resonator antenna with high port isolation for WiMAX and WLAN applications," *Int. J. RF Microw. Comput. Aided Eng.*, 2017.e21058.

[9] A.A. Khan, M. H. Jamaluddin, S. Aqeel, J. Nasir, J.R. Kazim, and O. Owais, "Dual-band MIMO dielectric resonator antenna for WiMAX/WLAN applications," *IET Microwaves, Antennas & Propagat.*, vol.11, no. 1, pp. 113-120, 2017.

[10] M.S. Sharawi, S.K. Podilchack, and Y.M.M. Antar, "A low profile dual-band DRA-based MIMO antenna system for wireless access points," *Proc. IEEE Int. Symp. on Antennas and Propagat. and USNC/URSI National Radio Science Meeting*, pp. 707-708, Vancouver, BC, 2015.

[11] A. Sharma, G. Das and R.K. Gangwar, "Design and analysis of tri-band dual-port dielectric resonator based hybrid antenna for WLAN/WiMAX applications," *IET Microwaves, Antennas & Propagat.*, vol. 12, no. 6, pp. 986-992, 2018.

[12] N.K. Sahu, G. Das and R.K. Gangwar, "Dual polarized tripleband dielectric resonator based hybrid MIMO antenna for WLAN/WiMAX applications," *Microw. Opt. Technol. Lett.*, vol. 60, no. 4, pp-1033-1041, 2018.

[13] N.K. Sahu, R.K. Gangwar, P. Kumari, "Dielectric Resonator Based Circularly Polarized MIMO Antenna for WLAN Applications," *Proc. Int'l Conf. on Microwave and Photonics* (ICMAP), Feb 9-11, 2018, DOI. 10.1109/ICMAP.2018.8354627.

[14] N.K. Sahu, G. Das, R.K. Gangwar, "L-shaped dielectric resonator based circularly polarized multi-input-multi-output (MIMO) antenna for wireless local area network (WLAN) applications," *Int. J. RF Microw. Comput. Aided. Eng.*, vol. 28, no. 9, 2018. DOI.10.1002/mmce.21426

[15] G. Das, A. Sharma, R.K. Gangwar, "Dielectric resonator based circularly polarized MIMO antenna with polarization diversity," *Microw. Opt.Technol.Lett.* vol. 60, no. 3, pp. 685-693, 2018.

[16] J. Iqbal, U. Illahi, M.I. Sulaiman, M. Alam, M. S. Mazliham, M.N. Yasin, "Mutual Coupling Reduction Using Hybrid Technique in Wideband Circularly Polarized MIMO Antenna for WiMAX Applications," *IEEE Access*, vol. 7, pp. 40951-40958, 2019.

[17] H.N. Chen, J. Song, J. Park, "A Compact Circularly Polarized MIMO Dielectric Resonator Antenna Over Electromagnetic Band-Gap Surface for 5G Applications," *IEEE Access*, vol. 7, pp. 1408889-140898, Sept. 2019.

[18] S.S. Singhwal, B.K. Kanaujia, A. Singh, J. Kishor, and L. Matekovits,"Multiple Input Multiple Output Dielectric Resonator Antenna with Circular Polarized adaptability for 5G Applications," *J. of Electromagnetic Waves and Applications*, Feb. 2020. DOI. 10.1080/09205071.2020.1730984

[19] R. Chowdhury, N. Mishra, M.M. Sani, and R.K. Chaudhary, "Analysis of a Wideband Circularly Polarized Cylindrical Dielectric Resonator Antenna With Broadside Radiation Coupled With Simple Microstrip Feeding," *IEEE Access*, vol. 5, pp. 19478-19485, 2017.

[20] D. Guha, P. Gupta, C. Kumar, "Dual band cylindrical dielectric resonator antenna employing $HEM11\delta$ and $HEM12\delta$ mode excited by new composite aperture," *IEEE Trans. Antennas and Propagat.*, vol. 63, no. 1, pp. 433-438, Jan. 2015.

[21] S.S. Singhwal, B.K. Kanaujia, A. Singh, J. Kishor, "Dual-port MIMO dielectric resonator antenna for WLAN applications," *Int. J. RF Microw. Comput.-Aided Eng.*, Dec. 2019. DOI.10.1002/mmce.22108

[22] M.S. Sharawi, "Printed multi-band MIMO antenna systems and their performance metrics," *IEEE Antennas and Propagat. Mag.*, vol. 55, no. 5, pp. 218–232, 2008.

[23] M.S. Sharawi,"Current Misuses and Future Prospects for Printed Multiple-Input, Multiple-Output Antenna Systems [Wireless Corner]," *IEEE Antennas and Propagat. Mag.*, vol. 59, no. 2, pp. 162-170, April 2017.

[24] M.S. Sharawi, S.K. Podilchak, M.U. Khan, and Y.M.M. Antar,"Dual-frequency DRA-based MIMO antenna system for wireless access points," *IET Microw. Antennas Propag.*, vol. 11 no. 8, pp. 1174-1182, 2017.